Int. J. Heat Mass Transfer. Vol. 35, No. 9, pp. 2257–2269, 1992
Printed in Great Britain

0017–9310/92 $5.00 + 0.00

Layer growth process of transient thermosolutal convection in a square enclosure

C. GAU, K. H. WU and D. J. JENG
Institute of Aeronautics and Astronautics, National Cheng Kung University, Taiwan, R.O.C.

(*Received* 16 *April* 1991 *and in final form* 22 *July* 1991)

Abstract—The rate of layer growth during thermosolutal convection in a square enclosure is studied both experimentally and analytically. The thermosolutal convection is induced by the combined thermal and solutal buoyancies which either augment or oppose each other. The layer growth process is attributable to the vertical solutal boundary flow which accumulates and stratifies along the horizontal wall. A mathematical model, based on the filling box process used to predict the layer growth rate, is developed. The solutal boundary flow that enters or exits the stratified layer is calculated by using an integral solution for natural convection due to combined thermal and solutal buoyancies along a vertical plate. Comparison of layer growth rate between the prediction and the data is made, and the agreement is excellent if the actual thickness of the solutal boundary layer flow at the inlet and the outlet of the stratified layer can be accurately determined. The actual thickness of the solutal boundary layer flow at the inlet and the outlet is found to increase with increasing buoyancy ratio.

1. INTRODUCTION

NATURAL convection flow caused by buoyancy forces resulting from temperature and concentration gradients is generally referred to as thermosolutal convection or double-diffusive convection. This kind of convection occurs commonly in natural as well as technological circumstances. In nature, thermosolutal convection caused by stable vertical concentration distribution with heating from the side or from the bottom has been widely investigated because of the interest in oceanography. Theoretical analysis based on stability theory is used to find the criteria explaining the occurrence of layered structures observed in the ocean. A brief survey of these problems is given by Turner [1]. In the technological circumstances, thermosolutal convection has many engineering applications, such as liquified natural gas storage, material processing and crystal growth processing. A summary of the techniques used for the growth of a crystal and a discussion of thermosolutal convection related to the process of crystal growth are provided by Ostrach [2].

Due to the interest in the transport process during growth of a crystal, a few experimental studies on the thermosolutal convection in shallow enclosures have been performed [3–6]. An elelectrochemical system is used to create a horizontal concentration gradient in the enclosure, which results in a convection due to a solutal buoyancy force other than the thermal one. A copper sulphate–acid solution is electrolysed to initiate cupric ion transport between the anode and the cathode. Three-layered flow structure can be initiated in the test cell due to the combined thermal and solutal buoyancies which either augment or oppose each other. These studies have found that the appearance of the layered structure depends on the buoyancy ratio and the aspect ratio of enclosures.

Lee and Hyun [7] have studied steady natural convection of salt water due to the simultaneously imposed horizontal temperature and concentration differences between the end walls in a low aspect ratio enclosure. Each end wall of the test cell is replaced by a membrane and a reservoir to supply fresh or salt water so that a constant concentration on the wall can be obtained. Multilayer flow structure at certain ranges of buoyancy ratio is also initiated. It is suspected that the occurrence of the layer may be due to the interaction of local thermal buoyancy and solutal stratification, as mentioned by Thorpe *et al.* [8].

To illustrate that the layer formation is not due to the interaction of thermal and solutal convection or the double-diffusive instability described by Thorpe, a pure solutal convection in the enclosure is performed [9]. At an earlier time, a thin layer along both the horizontal top and bottom walls is observed, which grows with time. Kamotani *et al.* [4] have explained, based on a visual observation, that the occurrence of the layer is due to thermal convection near the cold anode in the cooperating case, and near the cold cathode in the opposing case, that convects some of the lighter fluid into the region outside of the solutal boundary layer along the anode and causes the accumulation of the convected lighter fluid. The same explanation applies to the appearance of the bottom layer. However, Kamotani's viewpoint cannot explain the occurrence of the layer at an earlier time when the thermal convection inside the thin layer is not initiated, or when the buoyancy ratio is large and the thermal convection inside the stratified layer is entirely absent.

It appears that the observations and explanations

NOMENCLATURE

A	area
D	solutal diffusivity
F	Faraday constant
g	gravitational acceleration
H	height of enclosure
i	current density
k	thermal conductivity
L	length of enclosure
Le	Lewis number, α/D
m	mass or solutal gradient
$\dot{m}$	mass flow rate
M	molarity
N'	modified buoyancy ratio, $Ra_s^{*4/5}/LeRa_t$
Pr	Prandtl number, ν/α
q	ratio of boundary layer thickness
q_s''	mass flux, it_2/z_1F
Ra_s^*	modified solutal Rayleigh number, $g\beta_s q_s'' H^4/\nu D^2$
Ra_t	thermal Rayleigh number, $g\beta_t(T_h - T_c)H^3/\nu\alpha$
Sc	Schmidt number, ν/D
t	time
t_2	transference number of SO_4^{-2}
v	velocity component in the y-direction
v_v	characteristic velocity
W	width of enclosure
x	coordinate normal to the electrodes
y	coordinate parallel to the electrodes
y_0	layer thickness
z	coordinate normal to x and y axes
z_1	valency of cupric ion.

Greek symbols

α	thermal diffusivity
β	volumetric coefficient of expansion
γ	dimensionless layer thickness
δ	boundary layer thickness
η	dimensionless boundary layer thickness
θ	angle
ν	kinematic viscosity
ρ	density
τ	dimensionless time.

Subscripts

c	cold plate
h	hot plate
i, in	inlet
o, out	outlet
s	solutal convection
ss	steady state
t	thermal convection.

Superscripts

*	modified parameter or the stratified layer
-	mean value
''	flux.

of the initiation and growth of layers in the past are contradictory. The mechanism responsible for layer growth is not understood. Therefore, the objective of the present work is to experimentally and analytically study and find the mechanism for layer growth during thermosolutal convection. Experiments with flow visualization, concentration and temperature distribution measurements are performed [9]. The rate of layer growth at different buoyancy ratios is measured. The thermosolutal system used is the same as the one described in refs. [3–6]. However, the current density for initiation of electrolysis is maintained at a value less than half the limiting current condition. It has been shown experimentally in an isothermal tank that a constant mass flux boundary condition on the end wall can be achieved [10]. A mathematical model used to predict the rate of layer growth is derived and developed. The model prediction will be compared with the data.

2. EXPERIMENTAL APPARATUS AND PROCEDURE

The rectangular test cell was made of 20 mm thick plexiglass and had inside dimensions of 80 mm height, 80 mm width and 47 mm depth. Both the vertical side walls of the enclosure were made of 12 mm thick copper plate and served as both the electrodes and the heat sources/sinks. Two identically shaped rectangular heat exchangers were each bolted with and used for cooling and heating the copper plate, as shown in Fig. 1. The temperature of each of the copper plates was maintained uniform and controlled by a separate constant temperature bath that circulated heated or cooled water through the heat exchanger. The test cell and the experimental boundary conditions were made in such a way that a two-dimensional thermosolutal convection could be expected. To reduce heat loss to the environment, the test cell outside was insulated with 25 mm thick polystyrene foam. For flow visualization experiments, instead of using polystyrene an air gap was made outside and used for insulation. To further reduce the heat loss, the average temperature inside the test cell was maintained close to the room temperature.

To initiate electrolysis between the two electrodes, a d.c. power supply was used to provide the desired current. A digital multimeter and a recorder were connected in parallel to the electronic circuit to measure the temporal variation of the potential and the current, as shown in Fig. 2. To measure the surface temperature of the electrode, six Chromel–Alumel

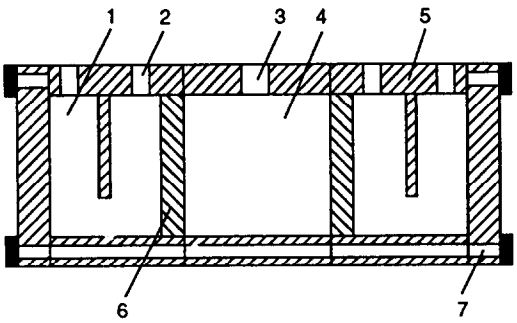

FIG. 1. Schematic diagram of enclosure: (1) heat exchanger, (2) circulation water inlet/outlet, (3) filling hole, (4) test cell, (5) plexiglass plate, (6) copper plate, (7) thread fastener.

thermocouples with wire diameter of 0.32 mm were embedded in each of the electrodes. All of the thermocouples embedded in the electrodes were connected to a data acquisition system used to record and print all of the temperatures.

The shadowgraph technique is used mainly to visualize the growth of the layer interface. The light beam from the 25 mW He–Ne laser was expanded with a spatial filter, which was then collimated with a large diameter plane convex lens. The collimated light passing through the region having large variation of refractive index was deflected and caused shadow on the screen. The salt finger structure and layer interface in the flow that had relatively large variation of refractive index could be clearly observed. A Nikon FM2 camera with a 55 mm microlens was used for photography.

Since the electrode surfaces can become roughened due to a long period of deposition of cupric ion, they can be readily detached from the test cell for polishing and cleaning. After the surface was cleaned, the prepared solution was carefully poured into the enclosure. Precautions were made to prevent air bubbles being entrapped inside. The entire test cell was placed on a platform which could be rotated and adjusted to ensure that the test cell was not tilted.

Before the experiment, the copper sulphate solution, having concentrations from 0.02 M to 0.1 M, was prepared. The amount of distilled water was measured with a graduated cylinder. The copper sulphate powder was carefully weighed on a precision electronic balance, which has an accuracy of ± 0.001 g, and was then mixed with a given amount of distilled water to reach a desired concentration. Finally, the H_2SO_4 solution was added into the mixed solution as a supporting electrolyte. The concentration of H_2SO_4 was 1.5 M. The thermal, chemical and transport properties of the solution are well documented in the paper of Wilke *et al.* [11].

To initiate the experiment, both the heated and the cooled water from each of the circulators were introduced, respectively, into the heat exchanger on the back of each electrode. Pure thermal convection was found to be well established after 3 h. The electrolysis in the solution was then initiated by switching on the d.c. power supply.

To maintain the current density at less than half the limiting current condition, the value of limiting current had to be measured before the experiment. The limiting current condition was determined by the potentiostatic–current method. The cell voltage was set with manual control in a stepwise manner, and the corresponding current was obtained and recorded. The procedure was repeated until a potential–current plateau was attained. To avoid the effect of ohmic overpotential in the test cell, a reference electrode was used to measure the cathodic limiting current. However, the limiting current condition was significantly affected by the temperature of the cathode, the temperature difference between the anode and the cathode, and the convection between the electrodes. Therefore, in the present studies, the limiting current condition was determined after pure thermal con-

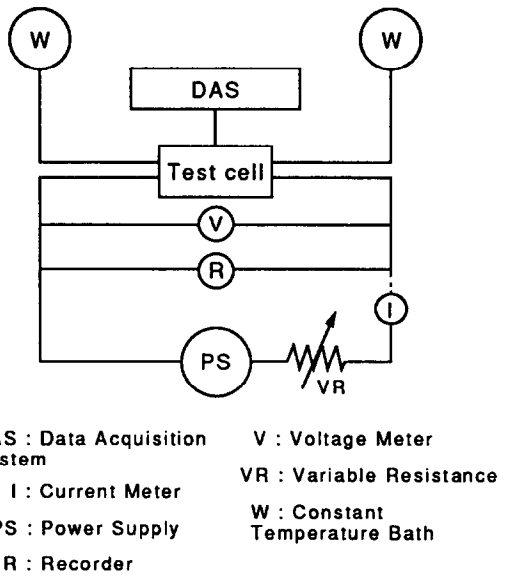

FIG. 2. Schematic diagram of the experimental set-up.

vection was well established. More details on the limiting current measurement can be found in ref. [11].

3. PHYSICAL DESCRIPTION OF THE LAYER GROWTH PROCESS

The process of layer formation and growth have been found for the case of pure solutal convection [9] and the case when the two vertical electrode surfaces on the sides are imposed with a finite temperature difference that is not large enough to produce a strong thermal convection destroying the layered flow structure [3–6, 9]. The experimental range for N' varies approximately from 0.5 to 10. Typical results of layer growth at different times are shown in Fig. 3. The flow visualization results, the concentration and the temperature distribution measurements in ref. [9] have suggested that the layer formation and growth is attributable to the fact that the lighter (heavier) fluid that comes from the solutal boundary layer accumulates and stratifies along the top (bottom) wall. The experimental results [9] suggest that the layer growth process in the current system is very similar to the density stratification process for a pure thermal convection in a confined region [12]. This phenomenon has been identified as the filling box process [1]. It appears that the layer growth rate in the current system can be predicted if the mass flow rate in the solutal boundary layer that enters or exits the stratified layer can be calculated.

In the system studied by Worster and Leitch [12], which is a pure laminar thermal convection in a cavity heated at one end, the development of the density stratification process, due to a vertical boundary layer flow along the heated wall which accumulates along the top wall, is studied both experimentally and analytically. Since the diffusion coefficient for the thermal is relatively large as compared with that for the solute, no sharp density front between the stratified region and the uniform bulk fluid is found as in the current system. During the experiments, different isotherms which descend in the tank are measured and used to represent the stratification process and the growth of the stratified region. The results of a similarity solution for convective boundary layers along a single heated plate are used to interpret quantitative features of the observed flow field and to develop an expression for the growth of the stratified region. In the stratified region, however, the momentum boundary layer is shown both analytically and experimentally to have approximately the same thickness as the thermal boundary layer. Therefore, the viscous flow outside the thermal layer is forced to move into the uniform bulk flow before entering into the stratified layer. The model used to predict the downward propagation of isotherms in the stratified region is compared with the results of a similarity solution. For the isotherms close to the edge of the stratified region, however, the discrepancy between the model and the similarity solution becomes large.

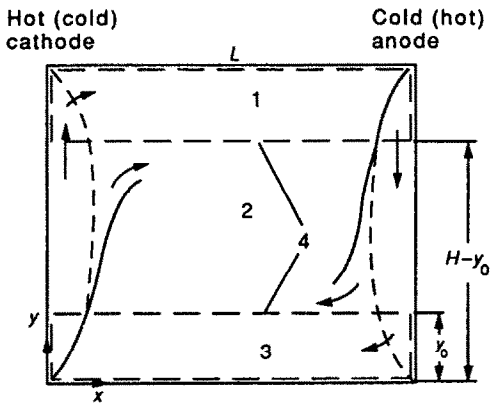

FIG. 3. Growth of layers at $t = 2.0$ h (a), $t = 4.0$ h (b) and $t = 6.0$ h (c) for augmenting convection with $N = 3.2$ and $Ra_L = 5.05 \times 10^7$.

In this report, we will extend the filling box concept used previously to the current system and develop a simple model to predict the layer growth process. The current flow system can be envisioned as shown in Fig. 4, where three different kinds of vertical boundary layers along the two vertical side walls are developed, i.e. the momentum, the thermal and the solutal boundary layers. Since the flow entering the stratified layer is solely from the solutal boundary layer flow, it appears that the development of the stratified layer in the current system is mostly due to the concentration stratification. Therefore, it can be concluded that the solutal stratification process can affect and restrict the momentum boundary layer flow that enters the stratified layer. In addition, it is expected that the well established thermal stratification can also affect and restrict the momentum boundary layer flow. The current experimental results for the layer growth measurement indicate that the thermal stratification can reduce the layer growth rate (this will be shown later in Figs. 5–8). The higher the thermal convection, the higher the thermal gradient in the bulk flow, and the slower the layer growth rate. It appears that the actual thickness for the momentum boundary layer flow entering the stratified layer is expected to be less than the solutal boundary layer thickness in a pure solutal convection. Therefore, in the solutally stratified layer it can be expected that, due to both the thermal and the solutal stratification, the three different boundary layers, i.e. the thermal, the solutal and the momentum boundary layers, have approximately the same thickness, which is less than the solutal boundary layer in a pure solutal convection. This has been confirmed by the flow visualization results in ref. [9], which indicate that due to the density stratification, the convective motion of fluid in both the top and bottom layers is very weak. To calculate the actual thickness for the momentum layer flow in the com-

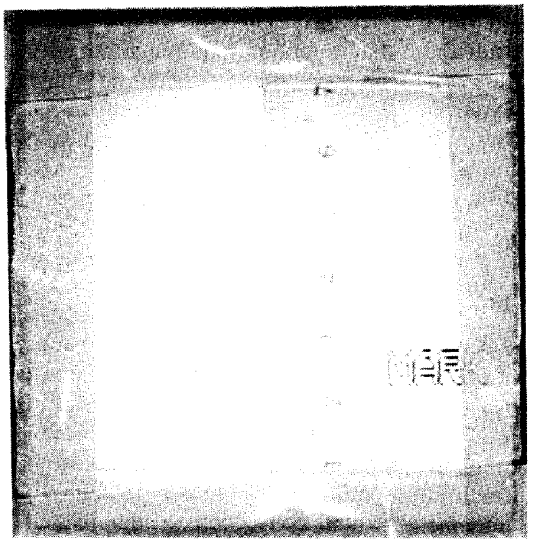

(a) t=2.0 hr.

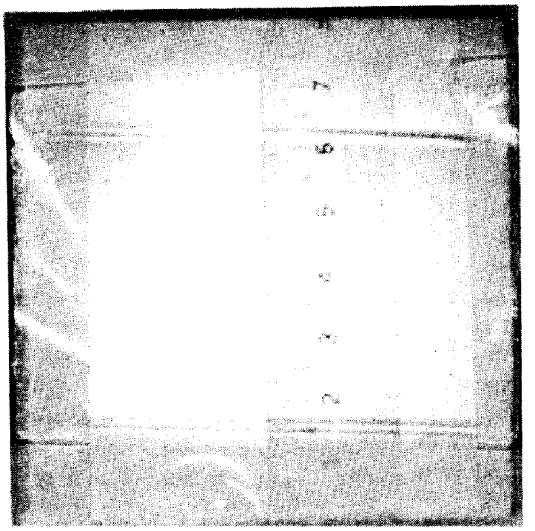

(b) t=4.0 hr.

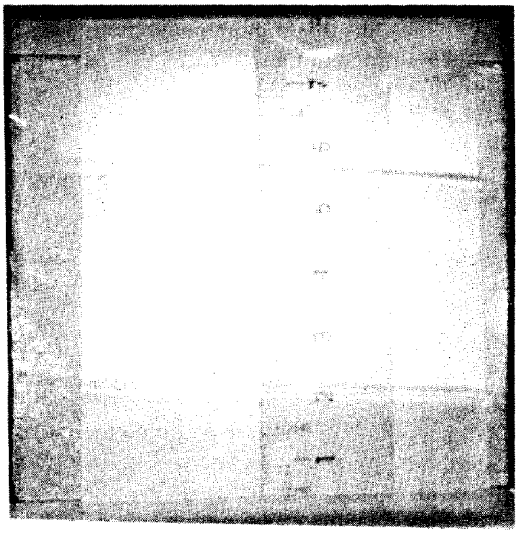

(c) t=6.0 hr.

FIG. 4. Schematic of layered flow model: (1) top layer, (2) uniform bulk fluid, (3) bottom layer, (4) layer interface.

bined thermal and solutal stratified layers, one needs to solve the coupled momentum, energy and species equations along a vertical plate in the combined thermal and solutal stratified regions. In addition, both the thermal and the solutal stratifications outside the boundary layers have to be provided. It appears that this is a difficult task to perform for the current system. Therefore, one would like to experimentally determine the actual thickness of the momentum boundary layer flow that enters or exits the stratified region. This will be discussed later.

4. MATHEMATICAL FORMULATIONS

The basic ideas used to develop a simple model for the layer growth has been partially described in the previous section. The schematic of the layered flow model is shown in Fig. 4. The dotted lines in Fig. 4 represent the solutal boundary layer flow. The viscous flow outside the solutal boundary layer, before entering the stratified layer, is forced to move into the uniform-solute bulk layer, in which the thermal boundary layer is in between the momentum and the solutal boundary layers. In addition to solutal layer flow into the stratified layer, the opposite boundary layer flow carries out the fluid inside the stratified layer and reduces the layer growth rate. For the opposed convection, the entire flow configuration is the same, except that the viscous flow outside the solutal layer, which is driven by the thermal buoyancy, is in the opposite direction. To simplify the analysis, it is assumed that the two solutal layer flows that enter and exist the top or the bottom layer, respectively, are separated so wide that they do not affect each other. In addition, the growth of the top layer is independent of the growth of the bottom one and vice versa. Therefore, the boundary layer flow along the vertical wall of the enclosure can be envisioned as the one along a single vertical plate. Therefore, the total mass flow that enters or exits the layer can be readily calculated.

All the thermophysical properties, except for the density that gives rise to the buoyancy, are assumed constant. The layer growth model can be formulated by selecting either the top or the bottom layer as a control volume. The rate of mass accumulated inside and the net rate of mass flow into the control volume must satisfy the law of mass conservation which is described mathematically as follows:

$$\bar{\rho}^* WL\frac{\mathrm{d}y_0}{\mathrm{d}t} = \left\{\int_0^x \rho v\,\mathrm{d}A\right\}_{y=H-y_0} - \left\{\int_0^{\delta_{vs}} \rho v\,\mathrm{d}A\right\}_{y=y_0}. \tag{1}$$

The first (second) term on the right-hand side of the above equation represents the rate of total mass flow entering (exiting) the stratified layer. Since the actual solutal boundary layer thickness in the stratified layer is not known, to calculate the mass flow into the stratified layer the boundary layer velocity profile is integrated to a desired location, which is to be determined experimentally. However, to calculate the mass flow out of the stratified layer, the boundary layer velocity is integrated to the edge.

In the calculation of the boundary layer mass flow that enters or exits the stratified layer, the integral method is used to obtain the boundary layer velocity distribution. The integral method has the advantage to readily obtain an analytical solution for the velocity, the temperature and the concentration distribution. The velocity distribution due to the combined thermal and solutal convection can be assumed to be any order of polynomials which satisfies the boundary condition. Since the rate of total mass flow entering or exiting the stratified layer is due to both the solutal and the thermal buoyancies, which are independent of each other, the velocity distribution for the combined convection can be assumed to be the sum of the polynomials, which is a velocity distribution of the flow due to pure thermal convection and the one due to pure solutal convection. For augmenting convection, the thermal buoyancy is assisted by the solutal one. Therefore, the total velocity in the solutal boundary layer can be written as

$$v = v_s + v_t \tag{2}$$

where v_s is the fluid velocity due to pure solutal buoyancy and v_t is the fluid velocity due to pure thermal buoyancy. For opposing convection, the thermal buoyancy is opposed to the solutal one. Therefore, the total velocity is written as

$$v = v_s|_{y=H-y_0} - v_t|_{y-y_0}. \tag{3}$$

For the current system, the Schmidt number of the fluid is very large ($Sc \simeq 2000$), while the Prandtl number is not so large ($Pr \simeq 7$). Therefore, the solutal buoyancy boundary layer is restricted to a very narrow region near the vertical wall, while the thermal layer is relatively large. Therefore, the fluid velocity distribution due to the solutal buoyancy can be assumed to be linear. We consider only the case for the augmenting convection. The total fluid velocity due to the combined thermal and solutal convection can be written as follows:

$$\begin{aligned} v &= v_{ys}\eta_s(1-\eta_s) + v_{yt}\eta_t \\ &= v_{ys}(1+f-\eta_s)\eta_s \end{aligned} \tag{4}$$

where

$$f = \frac{v_{yt}}{v_{ys}}q \tag{4a}$$

$$q = \frac{\delta_s}{\delta_t}. \tag{4b}$$

For the case of a pure thermal convection along a vertical flat plate with a uniform heat flux imposed, both the characteristic velocity v_{yt} and the thermal boundary layer thickness δ_t have been obtained analytically by Sparrow [13]. By using the analogy of heat and mass transfer, the characteristic velocity v_{ys} and

the solutal boundary layer thickness δ_s can be readily obtained. They are written in the following:

$$v_{yt} = C_{1t}x^{3/5} \tag{5a}$$

$$\delta_t = C_{2t}x^{1/5} \tag{5b}$$

$$C_{1t} = \nu\left(\frac{6000}{Pr}\right)^{1/5}(Pr+\tfrac{4}{5})^{-2/5}\left[\frac{g\beta_t q_t''}{\nu^2\alpha}\right]^{2/5} \tag{5c}$$

$$C_{2t} = \left(\frac{360}{Pr^2}\right)^{1/5}(Pr+\tfrac{4}{5})^{1/5}\left[\frac{g\beta_t q_t''}{\nu^2\alpha}\right]^{-1/5} \tag{5d}$$

$$v_{ys} = C_{1s}x^{3/5} \tag{6a}$$

$$\delta_s = C_{2s}x^{1/5} \tag{6b}$$

$$C_{1s} = \nu\left(\frac{6000}{Sc}\right)^{1/5}(Sc+\tfrac{4}{5})^{-2/5}\left[\frac{g\beta_s q_s''}{\nu^2 D}\right]^{2/5} \tag{6c}$$

$$C_{2s} = \nu\left(\frac{360}{Sc^2}\right)^{1/5}(Sc+\tfrac{4}{5})^{1/5}\left[\frac{g\beta_s q_s''}{\nu^2 D}\right]^{-1/5}. \tag{6d}$$

For the case of constant wall temperature and concentration condition in a uniform bulk fluid, the ratio of the characteristic velocity v_{yt} vs v_{ys} and the ratio of the boundary layer thickness δ_t vs δ_s have been derived from a scale analysis in the report by others [3, 14, 15], and they are

$$\frac{v_{ys}}{v_{yt}} \sim \left[\frac{N'}{Le}\right]^{1/2} \tag{7}$$

$$\frac{\delta_t}{\delta_s} \sim \begin{cases}[LeN']^{1/4} & \text{for } N' > 1\\ Le^{1/3} & \text{for } N' < 1.\end{cases} \tag{8}$$

Therefore, substituting equations (7) and (8) into equation (4a), one obtains

$$f = Le^{1/4}N'^{-3/4}. \tag{9}$$

For the case when a constant mass flux is imposed on the boundary, the modified buoyancy ratio N' is used [9], i.e.

$$N' = \frac{Ra_s^{*0.8}}{LeRa_t}. \tag{10}$$

To calculate the mass flow exiting the stratified layer, the boundary layer velocity distribution in the stratified layer would have a different form to that in the uniform bulk layer. In the stratified layer, the three different boundary layers, i.e. the thermal, the solutal and the momentum boundary layers, due to the density stratification are assumed to have the same thickness. Therefore, the boundary layer velocity distribution due to the solutal or the thermal buoyancy is assumed to be a second order polynomial which satisfies the boundary condition. Therefore, the total velocity distribution in the stratified layer due to the combined thermal and solutal convection can be written as follows:

$$\begin{aligned} v &= v_s^* + v_t^* \\ &= v_{ys}^*\eta_s^*(1-\eta_s^*) + v_{yt}^*\eta_s^*(1-\eta_s^*) \\ &= v_{ys}^*(1+f^*)(1-\eta_s^*)\eta_s^* \end{aligned} \tag{11}$$

where

$$f^* = \frac{v_{yt}^*}{v_{ys}^*} \tag{11a}$$

and

$$\eta_s^* = \frac{x}{\delta_{as}} \tag{11b}$$

and v_s^* is the boundary layer velocity in the pure solutal stratified layer, and v_t^* the velocity in the pure thermal stratified layer. Worster and Leitch [12] have demonstrated that for a pure thermal convection, the boundary layer velocity decreases with increasing thermal stratification in the bulk. Due to lack of information, however, the value of v_{yt}^*/v_{ys}^* is assumed to be equal to v_{yt}/v_{ys}, which is $(Le/N')^{1/2}$. The actual solutal boundary layer thickness δ_{as} is expected to be less than δ_s or δ_s^* and the relationship $\delta_{as} = C_1(N')\delta_s$ is assumed. In addition, the characteristic velocity in the pure solutal stratified layer v_{ys}^* is expected to be less than v_{ys} and the relationship $v_{ys}^* = C_2(m)v_{ys}$ is assumed, where m is the solutal gradient in the pure solutal stratified layer.

Substituting equations (4) and (11) into equation (1), the rate of growth of the stratified layer is

$$\begin{aligned} \bar{\rho}^* L\frac{dy_0}{dt} = &\left\{\bar{\rho}\delta_s v_{ys}\left[(1+f)\frac{\eta_s^2}{2} - \frac{\eta_s^3}{3}\right]\right\}_{in} \\ &-\left\{\tfrac{1}{6}\bar{\rho}\delta_s v_{ys}C_3(N')(1+f^*)\right\}_{out} \end{aligned} \tag{12}$$

where

$$\bar{\rho}\delta_s v_{ys} = \begin{cases} 18.49\bar{\rho}_i D_i Ra_{si}^{*1/5}\left(1-\dfrac{y_0}{H}\right)^{4/5} & \text{at the inlet} \\ 18.49\bar{\rho}_o D_o Ra_{so}^{*1/5}\left(\dfrac{y_0}{H}\right)^{4/5} & \text{at the outlet} \end{cases}$$

and $C_1(N')C_2(m) = C_3(N')$, which accounts for the ratios of boundary layer thickness and characteristic velocity. By a closer examination, $C_3(N')$ is actually the ratio of the exiting volume flow rate from the stratified layer vs that from the uniform layer. By using the non-dimensional parameters:

$$\tau = (18.49\bar{\rho}_i D_i Ra_{si}^{*1/5}/\bar{\rho}^* LH)t \tag{13a}$$

$$\gamma = \frac{y_0}{H}. \tag{13b}$$

Equation (12) can be non-dimensionalized as follows:

$$\frac{d\gamma}{d\tau} = F_i(1-\gamma)^{4/5} - F_o\gamma^{4/5} \tag{14}$$

where

$$F_i = (1+f)\frac{\eta_{si}^2}{2} - \frac{\eta_{si}^3}{3} \tag{15a}$$

$$F_o = \left(\frac{C_{4o}}{C_{4i}}\right)\frac{C_3(N')}{6}(1+f^*) \tag{15b}$$

$$\frac{C_{4o}}{C_{4i}} = \left(\frac{\bar{\rho}_o}{\bar{\rho}_i}\right)\left(\frac{D_o}{D_i}\right)^{3/5}\left(\frac{\nu_o}{\nu_i}\right)^{-1/5}\left(\frac{\beta_{so}}{\beta_{si}}\right)^{1/5}. \quad (15c)$$

To simplify the analysis, the property ratio C_{4o}/C_{4i} is assumed to be unity in the present experimental ranges covered. Once the values of η_{si} and $C_3(N')$ are determined, both F_i and F_o can be calculated, and equation (14) can be readily solved numerically to obtain the layer interface position at different times. However, both the values of η_{si} and $C_3(N')$ are not known and need to be determined from the experimental data.

The actual thickness for the solutal boundary layer flow that enters or exits the stratified layer is very thin and could not be readily measured. Therefore, it needs to be determined indirectly. The only information obtained, however, which is related to the actual boundary layer thickness for the mass flow in and out of the stratified layer is the layer interface position at different times. In the model equation, there are two unknowns, i.e. η_{si} and $C_3(N')$, which need to be determined. It appears that one needs to select two different boundary conditions from the information of interface position to determine the actual boundary layer thickness η_{si} at the inlet and the volume flow ratio at the outlet. The first boundary condition selected is at the initial stage ($\tau = 0$) where the layer growth rate is maximum. At this initial stage, the thickness of the stratified layer is zero, and only the mass flow in is related to the layer growth. The mass flow out does not contribute anything to the rate of layer growth. Therefore, the second term on the right-hand side of equation (14) can be eliminated. By measuring the layer growth rate at the initial stage, the value of η_{si} can be determined. The second boundary condition selected is at steady state when the layer growth rate is zero. At this stage, the rate of mass flow entering the stratified layer is equal to that exiting the layer. Therefore, the two boundary conditions selected and used to determine η_{si} and $C_3(N')$ are written in mathematical form as follows:

$$\text{at } \tau = 0, \quad \frac{d\gamma}{d\tau} = \tan\theta \quad (16a)$$

where θ is the angle between the slope of the curve for layer growth at $\tau = 0$ and the horizontal τ-axis;

$$\text{at } \tau = \tau_{ss}, \quad \frac{d\gamma}{d\tau} = 0. \quad (16b)$$

5. COMPARISON OF INTERFACE DATA WITH MODEL PREDICTION

Since the interface shape is tilted, an average interface position is determined by measuring the total volume of the stratified layer and dividing that value by the width of the enclosure. The dimensionless interface position γ measured vs dimensionless time τ for both the augmenting and the opposing convection is plotted in Figs. 5–8, respectively, and compared with the prediction. The agreement between the data and the prediction is found to be very good. The model can be used very accurately to predict the layer growth rate if the value of η_{si} at the inlet and the value of $C_3(N')$ at the outlet can be determined and provided.

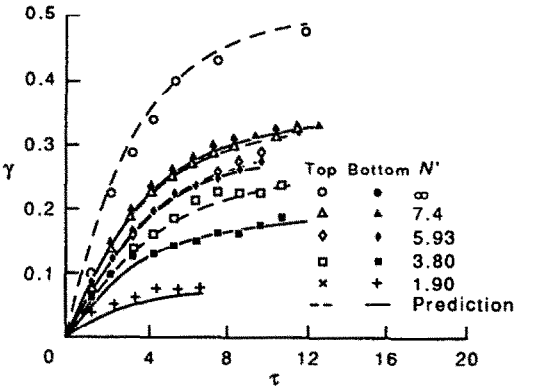

FIG. 5. Comparison of the layer growth between the data and the prediction for both the top and the bottom layer under augmenting convection.

Both the data and the prediction indicate that when the temperature difference between the two vertical side walls becomes large, which corresponds to a decrease in buoyancy ratio, the layer growth rate for both the augmenting and the opposing convection decreases. It appears that the thermal stratification can reduce the net rate of the solutal boundary layer flow into the stratified layer. This is attributed to the fact that thermal stratification occurring in the bulk can reduce the actual solutal boundary layer thickness. In addition, for the augmenting convection, the increase in temperature of the fluid causes a decrease in the viscosity and the density. This leads to an increase in the net rate of boundary mass flow entering into the top layer and causes an increase in the rate

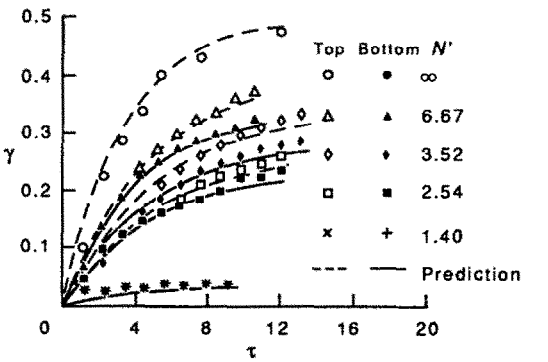

FIG. 6. Comparison of the layer growth between the data and the prediction for both the top and the bottom layer under opposing convection.

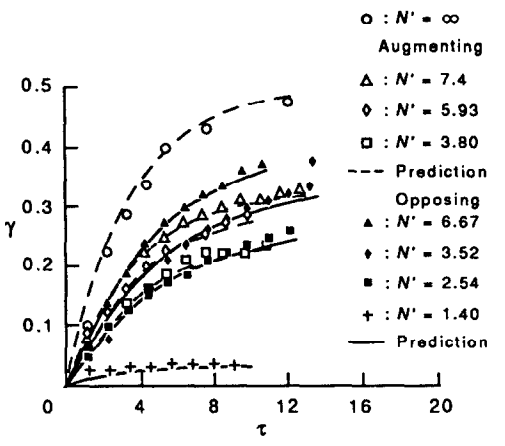

FIG. 7. Comparison of the growth of the top layer between the augmenting and the opposing convections.

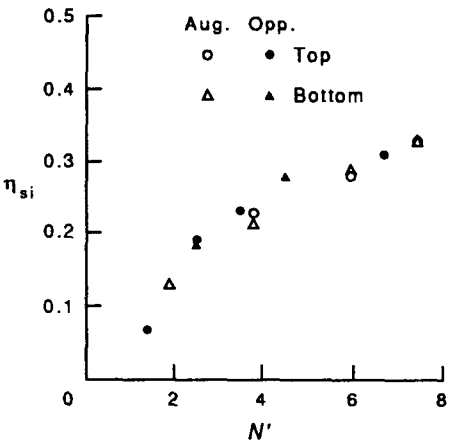

FIG. 9. Solutal boundary layer thickness at the inlet of the stratified layer.

of layer growth. For the case when $N' = 1.9$, the top layer is not initiated. This is attributed to the fact that the thermal stratification has become so large and the solutal layer thickness at the inlet has been reduced to such a small value that the mass flow rate exiting the stratified layer is greater than that entering the layer.

For the opposing convection at large buoyancy ratio, the decrease in the buoyancy ratio causes large deviation of layer growth rate between the top and the bottom layers, as shown in Fig. 6. The rate of growth of the top layer is much higher than the bottom one and even higher than the top layer for the augmenting convection, as shown in Fig. 7. This is attributed to the counter-flow motion and the mixing between the thermal and the solutal boundary layer flow which can effectively increase the net rate of solutal layer flow into the stratified layer. This will be discussed later. However, it appears that as the buoyancy ratio decreases further, as shown in Fig. 6, which corresponds to the increase in the temperature difference between the two vertical side walls, the heavy solutal boundary layer flow which enters the bottom layer is heated and causes a decrease in the viscosity and the density of the fluid. This leads to an increase in the velocity of the fluid and the rate of total volume flow into the bottom layer. Therefore, as N' decreases, the growth rate of the bottom layer approaches the top one. For the opposing convection, both the top and bottom layers appear even when the buoyancy ratio N' is very small ($N' = 1.4$). For the augmenting convection when $N' = 1.4$, the layered flow structure is not initiated. It appears that in comparison with the augmenting convection, the opposing one has the effect of increasing the net rate of solutal boundary flow into the stratified layer. The results in Fig. 7 clearly indicate that the layer growth rate for the opposing convection is higher than for the augmenting one. For the top layer, the discrepancy becomes small, as shown in Fig. 7, when the buoyancy ratio is small and the temperature difference between the two vertical walls increases, while for the bottom layer, the discrepancy becomes large, as shown in Fig. 8. Both the former and the latter are due to the decrease in viscosity and density of the fluid which increases the solutal layer flow into the stratified layer as the temperature of the fluid increases.

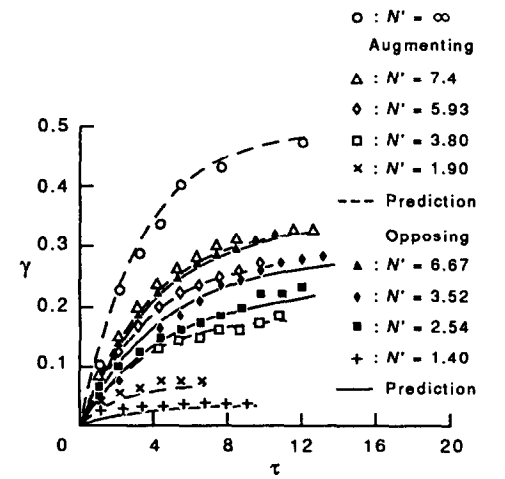

FIG. 8. Comparison of the growth of the bottom layer between the augmenting and the opposing convections.

6. EXPERIMENTAL RESULTS

The actual solutal layer thickness at the inlet η_{si} determined from experimental results is divided by the solutal layer thickness η_∞ with uniform bulk fluid outside, and their variation with the buoyancy ratio N' is shown in Fig. 9. For pure solutal convection, the results of $\eta_{si}/\eta_\infty = 0.8$ (which are not shown in Fig. 9 are obtained. This suggests that the solutal

stratification can restrict and reduce the solutal boundary layer flow. In addition, the value of $C_3(N')$ found is less than one. Therefore, the present results agree with the conclusion of Worster and Leitch [12] that the density stratification can reduce both the thickness and the velocity of the solutal boundary layer flow.

For the case with combined thermal and solutal convection, the results clearly demonstrate that in addition to the solutal stratification, the thermal stratification in the stratified layer can reduce the solutal boundary layer thickness, which leads to a reduction of the mass flow into the stratified layer and a slower rate of layer growth. It appears that a higher temperature difference across the two vertical side walls causes a higher vertical thermal gradient in the enclosure, which leads to a thinner solutal boundary layer. When the combined vertical thermal and solute gradient becomes so large that they completely restrict the solutal boundary layer flow, no layered flow structure can be obtained. It is estimated from Fig. 9 that for $N' \leqslant 1.2$, no layered flow structure or solutal boundary layer flow entering the stratified layer can exist. It is noted that the value of η_{si} for both the top and the bottom layer is the same, which increases with increasing buoyancy ratio N'. It appears that the two opposite solutal boundary layer flows, which enter the top and bottom layers, respectively, have the same thickness, and are symmetric with respect to the bulk flow, despite the density and the viscosity in both layers being significantly different.

For the opposing convection, the same value of η_{si} as that found for the augmenting convection is obtained, as shown in Fig. 9. It appears that although the thermal convection is opposed to the solutal one, the combined vertical thermal and solutal gradient created inside the stratified layer is expected to be the same as for the augmenting convection. In addition, due to the counter fluid motion and mixing of the two opposed boundary layer flows, part of the fluid in the solutal boundary layer is pushed to move into and be carried away by the thermal boundary layer flow. Since the fluid from the solutal boundary layer is less (more) dense than the thermal layer fluid near the cold cathode (hot anode), its motion has been identified by the shadowgraph as a salt-finger motion. The salt-finger motion is not observed for the case of augmenting convection. It appears that the portion of the solutal boundary layer flow moving into the thermal layer does not affect the solutal layer thickness inside the stratified layer. This is realized by the fact that the actual solutal boundary layer thickness in the stratified layer which is affected only by the density stratification is much smaller than the one in the uniform bulk layer. Therefore, the relatively slight variation of the solutal boundary layer flow in the uniform bulk layer does not affect the actual solutal layer thickness at the inlet of the stratified layer.

The values of $C_3(N')$ determined experimentally at the exit for both the augmenting and the opposing convections are shown in Fig. 10. The value of the volume flow ratio at the outlet is linearly proportional to the buoyancy parameter N'. The results clearly demonstrate that the thermal gradient inside the stratified layer can restrict and reduce the amount of actual solutal boundary layer flow, which is due to the decrease in boundary layer thickness and the fluid velocity inside the boundary layer. However, a large discrepancy is found for the value of $C_3(N')$ between the top and the bottom layers for both the augmenting and the opposing convections. By examining equation (15b), one concludes that this discrepancy is attributed to the assumption we made for C_{4o}/C_{4i}, which is the ratio of the physical properties at the inlet vs those at the outlet and is assumed to be unity. For the case of augmenting convection, the maximum value of C_{4o}/C_{4i} for the top layer can be 10% more, and that for the bottom layer can be 10% less. In addition, the greatest contribution for the value of C_{4o}/C_{4i} that is different from unity is due to the temperature. Therefore, for the case when ΔT between the hot and the cold walls is large, i.e. the value of N' decreases, the discrepancy of C_{4o}/C_{4i} between the top and the bottom layers becomes large. Therefore, to account for the variation of C_{4o}/C_{4i} with temperature, the value of $C_3(N')$ determined for the top layer can approach that for the bottom one.

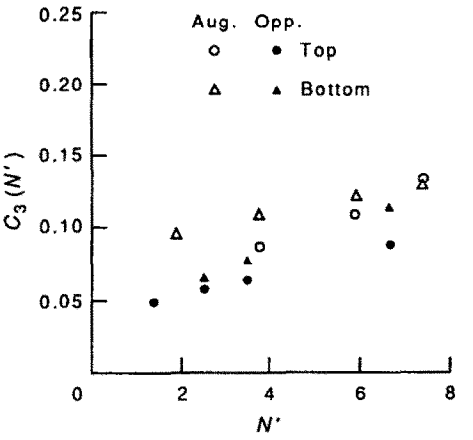

FIG. 10. Volume flow ratio at the outlet of the stratified layer.

However, a large difference of $C_3(N')$ in the top layer (or the bottom layer) between the augmenting and the opposing convection is found when a small temperature difference across the two vertical side walls is imposed. This is attributed to the counter-flow motion and the mixing in the uniform bulk layer between the solutal and the thermal boundary layer flows, for the opposing convection, which can restrict and reduce both the thickness and velocity of the solutal layer at the exit. However, since the actual solutal boundary layer in the stratified layer is much smaller than the one in the uniform bulk layer, the reduction in its thickness due to the counter-flow

motion in the uniform bulk layer is not expected. This has also been concluded in the discussion of η_{si}. Therefore, the reduction in $C_3(N')$ for the opposing convection is mainly due to the decrease in the boundary layer velocity which is caused by the opposed convection. For the case when ΔT between the hot and the cold walls is large, i.e. the value of N' decreases, the heavy solutal boundary layer flow near the anode can be heated, which causes a decrease in the density and the viscosity of the fluid. This leads to an increase in the net rate of volume flow into the bottom layer which makes the thickness of the bottom layer approach that of the top one. To account for the variation of C_{4o}/C_{4i} with temperature in equation (15b), the value of $C_3(N')$ determined for the top layer can be smaller than that for the bottom one when N' is small.

The values of F_i and F_o can be calculated from equations (15a) and (15b) once the values of η_{si} and $C_3(N')$ are obtained, since F_i and F_o are coefficients of the term $\gamma^{4.5}$ and the term $(1-\gamma)^{4.5}$, which can be used to calculate the layer growth rate. By examining equations (15a) and (15b), it is found that F_i is a function of N' and Le, and F_o is a function of N' and Le, and the ratio of the thermal physical properties at the inlet vs at the outlet C_{4o}/C_{4i}. In the present experiment, C_{4o}/C_{4i} is assumed to be unity and Le is a constant. Therefore, both F_i and F_o are functions of N' only. The variations of F_i and F_o with N' are calculated and plotted in Figs. 11 and 12, respectively.

The variation of F_i with N' is very much like the variation of η_{si} with N'. A unique function between F_i and N' can be obtained for each layer growing under augmenting or opposing convection. However, the variation of F_o with N' deviates for each layer growing under augmenting or opposing convection. F_o accounts for the ratio of the thermal physical properties at the inlet vs at the outlet of the stratified layer, which depends on the temperature and the concentration difference between the two vertical side walls. However, in the model equation the thermal physical properties are assumed to be constant. Therefore, a large difference in the F_o value between the top and the bottom layers for the augmenting convection can be expected. The difference in F_o value between the top and bottom layers increases, as shown in Fig. 12, when the temperature difference between the two vertical side walls increases, i.e. when the buoyancy ratio decreases. However, for the opposing convection, the difference in F_o value becomes small, especially when the temperature difference between the two vertical side walls increases, because the temperature effect on the thermal physical properties at the current stage is opposed to the concentration effect. However, the F_o value for the opposing convection is much smaller than that for the augmenting one. This is attributed again to the counter-flow motion and the mixing between the thermal and the solutal convection in the uniform bulk layer which can reduce the boundary layer velocity and cause a decrease in the mass flow rate at the outlet. Therefore, the layer growth rate for the opposing convection is much higher.

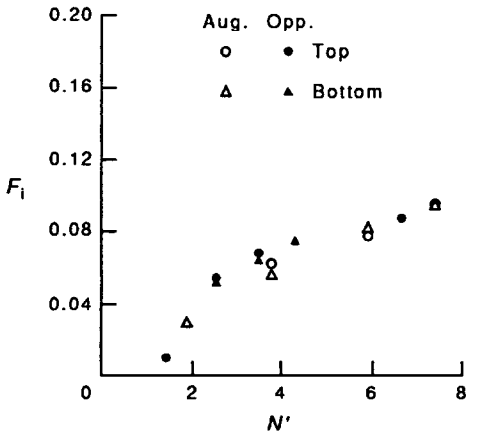

FIG. 11. Variation of F_i with buoyancy ratio at the inlet of the stratified layer.

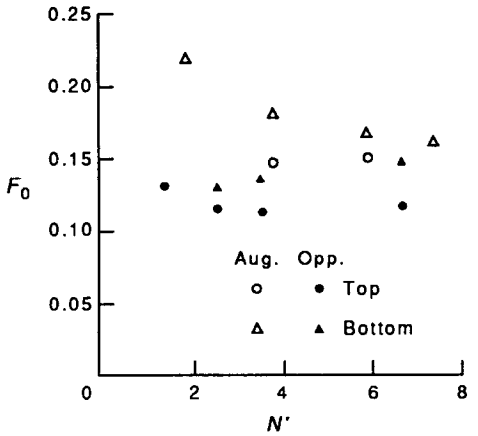

FIG. 12. Variation of F_o with buoyancy ratio at the outlet of the stratified layer.

7. CONCLUSIONS

The process of layer growth is actually the process of solutal stratification toward the core region and can be identified as the filling box process. The increase in the layer thickness is mainly due to solutal buoyancy which drives the lighter (heavier) fluid in the solutal boundary layer into the top (bottom) layer and causes the accumulation of fluid in the layer. In addition to the solutal boundary layer flow entering the stratified layer, the opposite boundary layer, which can move and carry out the fluid inside the stratified layer, reduces the layer growth rate. In addition, the rate of layer growth can be reduced by the well established

thermal stratification. The stronger the thermal convection, the higher the thermal gradient created in the bulk flow, and the slower the rate of layer growth. Therefore, the rate of layer growth increases with the buoyancy ratio. A mathematical model used to predict the layer interface motion is developed. The model can accurately predict the layer growth rate if the actual solutal boundary layer thickness η_{si} at the inlet and the volume flow ratio $C_3(N')$ at the outlet are provided. The values of η_{si} and $C_3(N')$ are both found to increase with increasing buoyancy ratio.

REFERENCES

1. J. S. Turner, Double-diffusive phenomena, *Ann. Rev. Fluid Mech.* **6,** 37–56 (1974).
2. S. Ostrach, Fluid mechanics in crystal growth—the 1982 Freeman scholar lecture, *J. Fluids Engng* **105,** 5–20 (1983).
3. L. W. Wang, Y. Kamotani and S. Ostrach, Experimental study of natural convection in a shallow horizontal cavity with different end temperatures and concentrations, Report FATS/TR-81-164, Case Western Reserve University (1983).
4. Y. Kamotani, L. W. Wang, S. Ostrach and H. D. Jiang, Experimental study of natural convection in shallow enclosures with horizontal temperature and concentration gradients, *Int. J. Heat Mass Transfer* **28,** 165–173 (1985).
5. S. Ostrach, H. D. Jiang and Y. Kamotani, Thermosolutal convection in shallow enclosures, *Proc. ASME/JSME Thermal Engng Joint Conf.*, pp. 158–169 (1987).
6. L. W. Wang and J. J. Chen, Flow patterns of thermosolutal convection in low aspect ratio enclosures, *Exp. Heat Transfer* **1,** 197–204 (1988).
7. J. Lee and M. T. Hyun, Experimental study of natural convection due to the combined buoyancy in a low-aspect ratio enclosure, *Proc. ASME/JSME Thermal Engng Joint Conf.*, pp. 209–213 (1987).
8. S. A. Thorpe, P. K. Hutt and R. Souisby, The effect of horizontal gradients on thermohaline convection, *J. Fluid Mech.* **38,** 375–400 (1969).
9. K. H. Wu, Experimental and analytical study of thermosolutal natural convection in square enclosures, Ph.D. thesis, Institute of Aeronautics and Astronautics, National Chen Kung University, Taiwan, R.O.C. (1991).
10. Y. Awakura, A. Ebata and Y. Kondo, Distribution of local current densities during copper electrodeposition on a plane vertical cathode, *J. Electrochem. Soc.* **126,** 23–30 (1979).
11. C. R. Wilke, M. Eisenberg and C. W. Tobias, Correlation of limiting current under free convection conditions, *J. Electrochem. Soc.* **100,** 513–523 (1953).
12. M. G. Worster and A. M. Leitch, Laminar free convection in confined regions, *J. Fluid Mech.* **156,** 301–319 (1985).
13. E. M. Sparrow, Laminar free convection on a vertical plate with prescribed non-uniform wall heat flux or prescribed non-uniform wall temperature, NACA TN3508 (1955).
14. A. Bejan, Mass and heat transfer by natural convection in a vertical cavity, *Int. J. Heat Fluid Flow* **6,** 149–159 (1985).
15. A. Bejan, *Convective Heat Transfer*, pp. 318–324. Wiley, New York (1984).

MECANISME DE CROISSANCE DE LA COUCHE D'UNE CONVECTION THERMOSOLUTALE VARIABLE DANS UNE CAVITE CARREE

Résumé—La vitesse de la croissance de couche pendant la convection thermosolutale dans une cavité carrée est étudiée expérimentalement et analytiquement. Cette convection est induite par les flottements thermique et solutal combinés qui s'allient ou s'opposent. Le mécanisme de croissance de couche est attribuable à l'écoulement vertical de frontière solutale qui s'accumule et se stratifie le long de la paroi horizontale. Un modèle mathématique basé sur le remplissage de boite est utilisé pour prédire la vitesse de croissance de couche. L'écoulement de couche solutale qui entre ou sort de la couche stratifiée est calculé par une solution intégrale pour la convection naturelle le long d'une plaque verticale. La comparaison des vitesses de croissance de couche calculées et expérimentales conduit à un accord excellent si l'épaisseur réelle de l'écoulement de couche limite solutale à l'entrée et à la sortie de la couche stratifiée peut être déterminée avec précision. Cette épaisseur augmente quand le rapport de flottement croît.

ÜBER DAS SCHICHTWACHSTUM BEI DER TRANSIENTEN DOPPELT-DIFFUSIVEN KONVEKTION IN EINEM QUADRATISCHEN HOHLRAUM

Zusammenfassung—Die Geschwindigkeit des Schichtwachstums bei der thermisch und konzentrationsgetriebenen Konvektion in einem quadratischen Hohlraum wird experimentell und analytisch untersucht. Die doppelt-diffusive Konvektion wird durch eine Kopplung der thermisch und konzentrationsbedingten Auftriebseffekte induziert, die sich entweder verstärken oder entgegenwirken. Der Vorgang des Schichtwachstums ist auf eine senkrechte Lösungsgrenzschicht zurückzuführen, die sich entlang der horizontalen Wand ansammelt und sich in Schichten aufbaut. Es wird ein mathematisches Modell entwickelt, das auf der "Filling Box"-Technik zur Bestimmung der Geschwindigkeit des Schichtdickenwachstums basiert. Die Strömung der Lösungsgrenzschicht, die in eine Schicht eintritt oder diese verläßt, wird mit einer integralen Lösung für die natürliche doppelt-diffusive Konvektion entlang einer senkrechten Platte bestimmt. Ein Vergleich zwischen berechneten und gemessenen Werten für die Geschwindigkeit des Schichtwachstums zeigt hervorragende Übereinstimmung, wenn die tatsächliche Dicke der Lösungsgrenzschicht am Eintritt und Austritt der Schichtung genau bestimmt werden kann. Es zeigt sich, daß diese Dicke mit wachsendem Auftriebsverhältnis zunimmt.

ПРОЦЕСС РОСТА СЛОЯ ПРИ НЕСТАЦИОНАРНОЙ КОНВЕКЦИИ ТЕПЛА И РАСТВОРЕННОГО ВЕЩЕСТВА В ПОЛОСТИ КВАДРАТНОГО СЕЧЕНИЯ

Аннотация—Экспериментально и аналитически исследуется скорость роста слоя в процессе конвекции тепла и растворенного вещества в полости квадратного сечения. Конвекция вызвана подъемными силами тепла и растворенного вещества, совместно действующими в одном или противоположных направлениях. Процесс роста слоя обусловлен вертикальным течением растворенного вещества в пограничном слое, которое накапливается и стратифицируется у горизонтальной стенки. Разработана математическая модель на основе процесса заполнения полости, используемого при расчете скорости роста слоя. Течение растворенного вещества, проникающее в стратифицированный слой и выходящее из него, определяется с помощью интегрального решения задачи естественной конвекции за счет совместного действия подъемных сил тепла и растворенного вещества вдоль вертикальной пластины. Сравнение расчетных и экспериментальных данных для скорости роста слоя обнаруживает очень хорошее согласие в случае, когда можно точно определить реальную толщину потока растворенного вещества в пограничном слое на входе и выходе из стратифицированного слоя. Найдено, что эта величина возрастает с увеличением отношения подъемных сил.